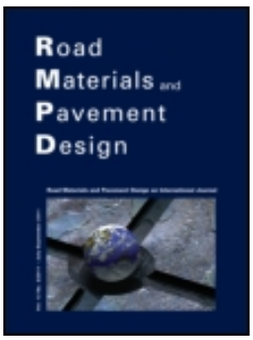

Road Materials and Pavement Design

ISSN: 1468-0629 (Print) 2164-7402 (Online) Journal homepage: https://www.tandfonline.com/loi/trmp20

# Moisture-induced strength degradation of aggregate–asphalt mastic bonds

Alex K. Apeagyei, James R. A. Grenfell & Gordon D. Airey

**To cite this article:** Alex K. Apeagyei, James R. A. Grenfell & Gordon D. Airey (2014) Moisture-induced strength degradation of aggregate–asphalt mastic bonds, Road Materials and Pavement Design, 15:sup1, 239-262, DOI: 10.1080/14680629.2014.927951

**To link to this article:** https://doi.org/10.1080/14680629.2014.927951

© 2014 The Author(s). Published by Taylor & Francis.

Published online: 19 Jun 2014.

Submit your article to this journal

Article views: 1506

View Crossmark data

Citing articles: 33 View citing articles

Full Terms & Conditions of access and use can be found at
https://www.tandfonline.com/action/journalInformation?journalCode=trmp20

*Road Materials and Pavement Design*, 2014
Vol. 15, No. S1, 239–262, http://dx.doi.org/10.1080/14680629.2014.927951

Taylor & Francis
Taylor & Francis Group

# Moisture-induced strength degradation of aggregate–asphalt mastic bonds

Alex K. Apeagyei*, James R. A. Grenfell and Gordon D. Airey

*Department of Civil Engineering, Nottingham Transportation Engineering Centre, University of Nottingham, University Park, Nottingham NG7 2RD, UK*

(*Received 30 July 2013; accepted 2 November 2013*)

A common manifestation of moisture-induced damage in asphalt mixtures is the loss of adhesion at the aggregate–asphalt mastic interface and/or cohesion within the bulk mastic. This paper investigates the effects of moisture on the aggregate–mastic interfacial adhesive strength as well as the bulk mastic cohesive strength. Physical adsorption concepts were used to characterise the thermodynamic work of adhesion and debonding of the aggregate–mastic bonds using dynamic vapour sorption and contact angle measurements. Moisture diffusion in the aggregate substrates and in the bulk mastics was determined using gravimetric techniques. Mineral composition of the aggregates was characterised by a technique based on the combination of a scanning electron microscope and multiple energy dispersive X-ray detectors. Aggregate–mastic bond strength was determined using moisture-conditioned butt-jointed tensile test specimens, while mastic cohesive strength was determined using dog bone-shaped tensile specimens. Aggregate–mastic bonds comprising granite mastics performed worse in terms of moisture resistance than limestone mastic bonds. The effect of moisture on the aggregate–mastic interfacial bond appears to be more detrimental than the effect of moisture on the bulk mastic.

**Keywords:** asphalt mastic; adhesive strength; bitumen; diffusion; moisture-induced damage

## 1. Introduction

One of the most important factors influencing the durability of asphalt mixtures designed for pavement construction is moisture-induced damage. A common manifestation of moisture-induced damage is a loss of cohesion in the mixture and/or loss of adhesion between the bitumen and aggregate interface (Airey & Choi, 2002) or more realistically, a loss of adhesion at the aggregate–asphalt mastic interface and/or cohesion within the bulk mastic (Airey, Masad, Bhasin, Caro, & Little, 2007).

The actual mechanism of moisture-induced damage is, however, not completely understood but the phenomenon is believed to be governed in part by the physico-chemical interactions between mastic and aggregates, in the presence of water. The build-up of an interfacial water layer several monolayers thick (35–45 nm) at the aggregate–bitumen interface has been cited as a major cause of adhesion loss (Nguyen, Byrd, Alsheh, & Bentz, 1995). It has been shown (Airey et al., 2007) that the mineralogical and chemical composition of aggregates may play a fundamental and more significant role in the generation of moisture damage, than bitumen properties such as penetration grade, acid number, and molecular size distribution. The same study showed that surface energy

*Corresponding author. Email: alex.apeagyei@nottingham.ac.uk

© 2014 The Author(s). Published by Taylor & Francis.
This is an Open Access article distributed under the terms of the Creative Commons Attribution License (http://creativecommons.org/licenses/by/3.0), which permits unrestricted use, distribution, and reproduction in any medium, provided the original work is properly cited. The moral rights of the named author(s) have been asserted.

measurements and associated bond energy calculations can be used as an effective tool to identify bitumen–aggregate pairs that are susceptible to moisture-induced damage. Thus, the mechanism of moisture-induced damage in asphalt mixtures can be better understood if the mineralogical composition of aggregates as well as the physico-chemical characteristics of aggregate and mastics can be linked with the aggregate–mastic mechanical bond strength.

This paper presents a study of moisture-induced strength degradation of aggregate–mastic joints subjected to various moisture conditioning regimes at 20°C for extended conditioning times. The differences in the resistance to the effect of moisture on various aggregate–mastic specimens were explained using multiple adhesion theories as well as the differences in mineralogy of the aggregates used. Most current studies do not relate the magnitude of the interfacial water to bond strength but rather relate bond strength degradation with moisture conditioning time. In this study, the quantity of water at the aggregate–mastic interface was determined by applying Fick's diffusion model to moisture transport to the aggregate–mastic interface via the granite aggregate substrate and analysing the results to establish relationships between bond strength and moisture concentration.

## 2. Theories

### 2.1. *Fick's diffusion model*

Diffusion can be defined as the movement of molecules from a region of high concentration to a region of low concentration. Diffusion is considered to be one of the key modes of moisture transport in pavements that influence durability of asphalt mixtures. Diffusing moisture can cause pavement deterioration in two general ways: (1) by attacking and weakening the adhesive bond between asphalt mastic and aggregate and (2) by degrading the cohesive strength of the asphalt mastic. By measuring the diffusion coefficient of asphalt mastics and of aggregates, the effect of moisture on pavements deterioration can be modelled numerically in order to better understand the moisture damage phenomenon.

Moisture diffusion in asphalt mixtures is usually characterised by using the diffusion coefficient parameter (Apeagyei, Grenfell, & Airey, 2013; Arambula, Caro, & Masad, 2010; Caro, Masad, Bhasin, & Little, 2008; Kassem, Masad, Bulut, & Lytton, 2006; Kringos, Scarpas, & deBondt, 2008; Vasconcelos, Bhasin, Little, & Lytton, 2011). The theoretical bases for moisture coefficient determination are Fick's laws which assume that for an isotropic material, (1) the steady-state rate of transfer of a diffusing substance through a unit cross-sectional area is proportional to the concentration gradient measured normal to the section (Equation (1)) and (2) the rate of change of concentration of the diffusing substance under unsteady state conditions is proportional to diffusion coefficient (Equation (2)). The solution to the differential equation in Equation (2) for a sample with planar infinite geometry is given by Equation (3). Using the moisture uptake data and Equation (3), moisture diffusion coefficient values for the mastics and aggregate substrates used in this study were estimated.

$$F = -D\frac{\delta C}{\delta x}, \tag{1}$$

where $F$ is the rate of transfer per unit area of section (flux); $D$ the diffusion coefficient; $C$ the concentration of the diffusing substance; and the space coordinate measured perpendicular to the section (Crank, 1975)

$$\frac{\delta C}{\delta t} = -D\frac{\delta^2 C}{\delta x^2}, \tag{2}$$

where $t$ is the time

$$\frac{M_t}{M_\infty} = 1 - \sum_{n=0}^{\infty} \frac{8}{(2n+1)^2\pi^2}\, \mathrm{e}^{-D(2n+1)^2\pi^2 t/l^2}, \tag{3}$$

where $M_t$ is the moisture uptake at time $t$, $M_\infty$ the equilibrium moisture uptake, $l$ the specimen thickness, and $n$ an integer.

A moisture uptake profile describes the relationship between the amount of moisture ($M_t$) a hygroscopic material exchanges (absorbs or desorbs), at a given relative humidity (RH) and temperature, with time. If $w_0$ is the initial (dry) mass of a given material and $w_t$ is the mass after time $t$, then the moisture uptake can be computed as the ratio of the amount of moisture absorbed at a given time to the initial dry mass of the sample at the of beginning the test (Equation (4)). For a material at a given temperature and RH, moisture uptake increases until it reaches a thermodynamic equilibrium at which point no further changes in moisture uptake occur. The moisture content at thermodynamic equilibrium ($M_\infty$) is called the equilibrium moisture uptake

$$\text{Mass uptake (\%)} = M_t = \frac{w_t - w_0}{w_0}. \tag{4}$$

### 2.2. *Adhesion theories*

As previously mentioned, asphalt mastic can be considered as the main adhesive that binds the aggregates in a mix together. Therefore, in order to better understand the moisture damage problem, it is essential to appreciate some of the concepts behind the adhesion and debonding processes. Several adhesion theories have been proposed in the past. They include the physical adsorption theory, chemical bonding theory, diffusion theory, electrostatic interactions theory, mechanical interlocking theory, and weak boundary layer theory (Wake, 1978). For asphalt mixtures, the first two theories might be the most relevant as discussed next.

Key concepts of the physical adsorption theory include: (1) adhesive and substrate are in intimate contact and van der Waals forces operate between them, (2) van der Waals forces consists of two components – polar and dispersion – which could be evaluated by using contact angle and vapour sorption measurement techniques, and (3) thermodynamic work of adhesion, calculated using the two component van der Waals forces, can be used to assess the stability of the bond between an adhesive and a substrate (Wake, 1978). Adhesive–substrate bonds with positive thermodynamic work of adhesion are considered stable, while bonds with negative work of adhesion are considered unstable. One manifestation of damage for a bond with a negative work of adhesion in the presence of water is an irreversible loss of bond strength. For asphalt mixtures, concepts based on the physical adsorption theory is currently the most widely used method (Bhasin, Masad, Little, & Lytton, 2006). The basis for this could be attributed to the fact that the bond between bitumen and aggregate involves intimate contact between thin films of asphalt and aggregates during mixing.

The formation of covalent, ionic, or hydrogen bonds across an adhesive–substrate interface is the basis for the chemical bonding theory of adhesion (Wake, 1978). The interfacial force due to ionic pairs is given by Equation (5) (Comyn, 2005) where $q_1$ and $q_2$ are the ionic charges; $\varepsilon_0$ the permittivity of a vacuum; $\varepsilon_r$ the relative permittivity of the medium; and $r$ the inter-ionic distance.

$$F = \frac{q_1 q_2}{4\pi \varepsilon_0 \varepsilon_r r^2}. \tag{5}$$

Water at ambient temperatures has a very high relative permittivity of 80. The corresponding relative permittivity of bituminous materials, however, are quite low with reported values in the range of 2.6–2.8 for bitumen, 4.0–4.6 for newly constructed dry asphalt pavements, and 6–8 for wet or moisture damaged pavements (Chang, Chen, Wu, 2011; Evans, Frost, Stonecliffe-Jones, & Dixon, 2007; Saarenketo, 2013; Vlachovicova, Stastna, & Zanzotto, 2003). Since an approximately linear relationship exists between the relative permittivities of mixtures of water and

organic solvents and mixture composition (Comyn, 2005; Bottcher, 1973; Sihvola, 1999), the high $\varepsilon_r$ of water means even small amounts of absorbed water in the adhesive can cause a large increases in $\varepsilon_r$ and a reduction in $F$. The reduction in $F$ due to moisture absorption by an adhesive is reversible; hence complete removal of water (say by drying) from an adhesive joint can restore $F$ to the original value. Thus, the major difference between the adsorption theory and the chemical bond theory of adhesion is that the latter permits partial recovery of damage in a wet adhesive bond when the bond is dried, while the former determines whether an adhesive bond is stable or not stable (zero strength) in the presence of water.

On the basis of the aforementioned adhesion theories, several possible mechanisms by which the bond between an adhesive and a substrate can be damaged by moisture are obvious. Moisture can weaken the adhesive bond by (1) causing reversible changes in the adhesive properties as exemplified by recovery of joint strengths in previously wet joints; (2) causing irreversible changes in adhesive properties leading to cracking, crazing, or hydrolyses; (3) attacking the adhesive–substrate interface by displacing or weakening of van der Waals interactions leading to a reduction in the thermodynamic work of adhesion; and (4) causing swelling in the adhesive and or the substrates leading to swelling stresses (Comyn, 1983). The reversible changes in adhesive properties (strength, stiffness, etc.) with moisture could be explained by the chemical bonding theory, while the physical adhesion theory could explain most of the other mechanisms of moisture damage. Reversible loss of adhesion could also be attributed to plasticisation (decrease in glass transition temperature) of the adhesion by water. In the latter case, the Fox equation (Fox, 1956) could be used to estimate, approximately, changes in glass transition temperature. For most adhesive bonds, it is conceivable to expect a combination of the various damage mechanisms to occur simultaneously. This is the approach adopted in this study to investigate the moisture damage problem.

## 3. Materials and methods

### 3.1. *Aggregates*

Samples of limestone and granite mineral aggregates, aggregate boulders, and mineral fillers were obtained from various UK quarries. Data from previous studies (Airey et al., 2007) suggest that asphalt mixtures fabricated from these aggregates exhibit significantly different moisture sensitivity under laboratory conditions. Therefore, it was expected that mastic specimens made from the selected aggregates would show different moisture-induced strength degradation with time. The aggregates for the mastics were mechanically sieved in the laboratory to obtain only materials passing the 1-mm sieve and retained on 0.125-mm sieve (fine aggregate). In addition to the fine aggregates, limestone and granite mineral fillers satisfying BS EN 1097-7-2008 were used. Again, the choice of the mineral fillers was made to quantify the effect, if any, of different types of fillers used in asphalt mixtures.

As previously discussed, the mineralogical compositions of aggregates are believed to have a profound influence on moisture damage susceptibility of asphalt mixtures. The mineralogical compositions of the aggregates were characterised using a Mineral Liberation Analyzer (FEI Quanta 600 SEM). The device combines an automated Scanning Electron Microscope and multiple Energy-Dispersive X-ray detectors with state-of-the-art analysis software to produce quantitative mineralogy measurements. The results were used to identify key mineral phases and their influence on the moisture-induced aggregate–mastic adhesive strength degradation.

Surface characteristics such as porosity, specific surface area, and surface free energy (SFE) are key physico-chemical properties of aggregates that influence the adhesion strength of asphalt mixtures. The physico-chemical properties of samples of the aggregates were characterised using

a dynamic sorption device (DVS Advantage). The technique involved exposing aggregate samples to varying concentrations (partial vapour pressures) of carefully selected probe liquids and measuring the mass gain with time using a sensitive microbalance (0.1 μg). The probe liquids used included chloroform, ethyl acetate, and octane. Detailed discussion of the sorption technique is provided elsewhere (Grenfell et al., 2013, 2014). The results were used to generate a series of sorption isotherms from which the Brunauer, Emmett and Teller (BET)-specific surface area and SFE components of the aggregates were estimated. The results were also used to estimate the relative porosity of the aggregates, and the thermodynamic work of adhesion and debonding of the aggregate–bitumen bond. The estimated intrinsic work of adhesion was compared with the practical work of adhesion obtained through tensile butt-joint specimen testing.

Another important parameter that influences moisture-induced damage in asphalt mixtures is the rate and amount of water absorption of the aggregates. Moisture absorption tests were conducted to simulate moisture transport in the aggregate substrates using a total water immersion method at a temperature of 20°C. The approach involved submerging uncoated aggregates disks with nominal dimensions 23 mm diameter by 15 mm thick in deionised water and measuring moisture uptake using a sensitive microbalance (0.1 μg resolution). The data (mass uptake and conditioning time) were fitted to a Peleg-type model as shown in Equation (6) (Peleg, 1988). The model parameter $C_1$ represents the rate of moisture uptake, while $C_2$ is a measure of the equilibrium moisture content (reciprocal of the maximum water uptake). The results were compared with the aggregate–mastic bond strength in an attempt to quantify the effect of water on bond strength degradation. Moisture uptake profiles were computed as the ratio of moisture uptake at a given time to the original dry weight of the sample at the beginning of the test (Equation (4)). The moisture uptake versus conditioning time data also enabled the estimation of an apparent moisture diffusion coefficient. Apparent moisture diffusion coefficient $D$ of the aggregate substrate was estimated assuming Fickian diffusion (Equation (7)) based on the moisture uptake profiles, where $l$ is the thickness of the aggregate substrate and $t_{0.5}$ the time to reach one half of the maximum water uptake.

$$M_t = \frac{t}{C_1 + t^* C_2}, \tag{6}$$

$$D = 0.049\left(\frac{l^2}{t_{0.5}}\right). \tag{7}$$

An error function-based numerical model (Bell & Labuza, 2000) was applied to characterise the transport of water in both aggregates, bulk mastic, as well as the interfacial moisture content variation with time and its influence on stiffness degradation. The models are based on the assumption that when two solids ($X$ and $Y$) with dissimilar but uniform moisture concentrations $m_x$ and $m_y$ are put in perfect contact, Equations (8) and (9) could be used to describe moisture distribution with time. Provided the aforementioned conditions hold, then under steady-state conditions, the concentration of water at the interface ($m_{int}$) can be approximated by Equation (10). Here, $D$ is the moisture diffusion coefficient, $l$ the characteristic thickness, erf the error function, and subscripts $x$ and $y$ refer to material $X$ and $Y$, respectively,

$$\frac{m_x - m_{ix}}{m_{e_x} - m_{i_x}} = \mathrm{erf}[0.5 l_x (D_x)^{-0.5}], \tag{8}$$

$$\frac{m_y - m_{iy}}{m_{e_y} - m_{i_y}} = \mathrm{erf}[0.5 l_y (D_y)^{-0.5}], \tag{9}$$

$$\frac{m_x - m_{int}}{m_{int} - m_y} = \left(\frac{D_y}{D_x}\right)^{0.5}. \tag{10}$$

### 3.2. *Asphalt mastics*

Four asphalt mastics were fabricated for testing using the same bitumen but two fine aggregates (GA for granite or LA for limestone) and two mineral fillers (GF for granite or LF for limestone). The proportion of the constituent components (fine aggregate, mineral filler, and bitumen) of the mastics used was 50:25:25 by weight of mixture and was chosen to mimic mastic mix design typically used in open-graded friction course asphalt mixtures in the Netherlands (Kringos et al., 2008). A 40/60 pen grade from a single source was used for preparing all the mastics. The bitumen is typical of those that are commonly used for asphalt mixture production in the UK with a reported total SFE of about 31 $mJ/m^2$ (Grenfell et al., 2013, 2014). The mastics were produced by combining the dried aggregates and molten bitumen using a Hobart mechanical mixer at a mixing temperature of 185°C. The mastics were then put in quart tins and stored in temperature-controlled (20°C, 50% RH) conditions until testing. The bulk specific gravity of the mastics was estimated to be approximately 1.917.

Similar to the aggregate substrate, the moisture absorption characteristics of the mastics were determined by submerging samples under water at 20°C and monitoring moisture uptake using a microbalance. Unlike the aggregates, samples for the mastic water absorption were dog bone shaped with dimensions 17.75 mm at the middle, 21 mm at the top, and 62 mm tall and the tests lasted for almost 90 days. Apparent moisture diffusion coefficient $D$ of the mastics was estimated assuming Fickian diffusion (Equation (3) and a semi-finite specimen of thickness 17.75 mm (gross approximation). The results were used to model moisture diffusion from the aggregate substrate through the interface to the mastic with time using Equations (8)–(10).

### 3.3. *Adhesion tests*

#### 3.3.1. *Adhesion tests – aggregate substrate fabrication*

Samples of granite boulders that were used for making the aggregate substrates were obtained from a local rock quarry and transported to the lab. Once in the lab, several 23-mm diameter cores were obtained from the boulders. The cores were then saw-cut using a water-cooled tile saw with carbide-tipped blade into disk-shaped substrates measuring approximately 23 mm diameter by 15 mm thick. The top and bottom surfaces of the substrates were polished using No. 5 sandpaper, to remove all blemishes left by the sawing process, in order to ensure parallel surfaces necessary for accurate adhesion testing. The fabrication of the substrates was completed by washing the substrates in deionised water (25°C) and then drying them in an oven at 70°C for 48 h.

Only about 70 substrates were fabricated using the above procedures because of lack of materials. The 70 substrates were deemed sufficient to fabricate enough butt-jointed aggregate–mastic specimens for the first three moisture conditioning steps (0, 1, and 7 days) for the four mastic types. It was anticipated that the substrates used for the three conditioning cycles would be cleaned and reused for additional testing beyond seven days. Thus, the rest of the substrates were obtained by cleaning the used aggregate substrates. The mastic-coated aggregates were cleaned using acetone followed by a thorough rinse in deionised water. Initially, this approach was considered adequate for restoring the aggregate substrates to their original state. However, as would be discussed later, it appears that the cleaned aggregates had water absorption properties that were different from the virgin aggregate.

#### 3.3.2. *Adhesion tests – adhesion specimen fabrication and moisture conditioning*

The substrates and mastic were heated to a temperature of 140°C. Small amounts of mastic were then poured into silicone moulds to form mastic films of dimensions approximately 3 mm thick and about 26 mm diameter. The idea was to produce a mastic film with an aspect ratio (diameter

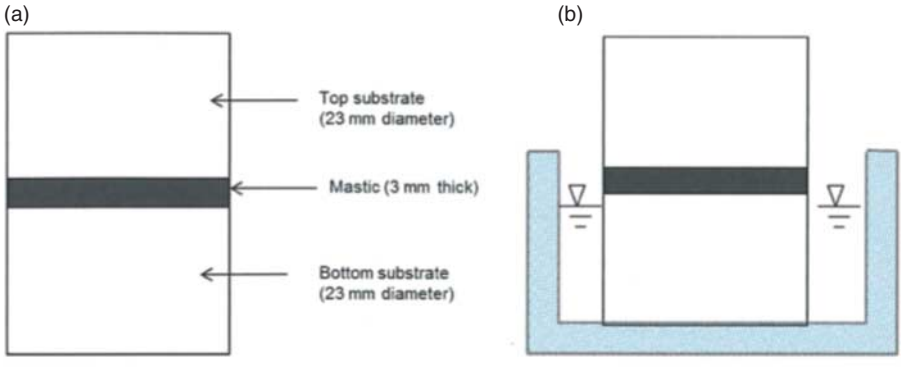


Figure 1. (a) Adhesion test specimen showing butt-jointed specimens consisting of 3-mm thick asphalt mastic sandwiched between two 15-mm thick by 23 mm diameter aggregate substrates. (b) Specimen with bottom substrate partially submerged to ensure water enters aggregate–mastic interface before entering bulk mastic material.

to thickness ratio) of about 8. The mastic films were annealed to the 23 mm diameter hot (130°C) aggregate substrates. A second aggregate substrate, also at 130°C, was annealed to the exposed face of the mastic to form a butt joint comprising the 3-mm thick mastic sandwiched between two aggregate substrates. The whole assembly (mastic sandwiched between two aggregate substrates) was trimmed using a hot knife to produce the tensile butt-jointed specimens (Figure 1(a)). The specimens were then kept at 70°C for 2 h to ensure complete bonding. An aluminium-backed adhesive film was used to cover the mastic film during the 2-h period to ensure that no material leaked out of the mastic. At this stage, the specimens were either stored dry or moisture conditioned and then tested.

Moisture conditioning was performed at 20°C by partially submerging substrate in water such that only about 1–2 mm of the bottom aggregate substrate was exposed to open air (Figure 1(b)). The arrangement ensured that the aggregate–mastic interface was completely dry at the beginning of a test and, therefore, moisture reached the aggregate/mastic bond only through the aggregate. Thus, the potential for moisture-induced adhesive failure was enhanced as the interface (not the bulk mastic) was in direct contact with the diffusing water during the duration of the moisture conditioning.

### 3.3.3. *Adhesion tests – aggregate-mastic interfacial bond strength*

The aggregate–mastic interfacial bond strength was determined with a bespoke tensile testing rig mounted on an Instron testing machine (Figure 2). A constant cross-head speed of 20 mm/min was applied. All the tests were conducted at a constant temperature of 20°C. To determine the effect of conditioning time on strength degradation of the aggregate butt joints, three conditioning times (0, 1, and 7 days) were used. Three replicate specimens were tested for each combination of aggregate substrate and mastic combination. About 36 butt-jointed specimens were thus tested. Additional specimens were tested to investigate the effect of moisture absorption on adhesive strength degradation of substrates that had already been coated with mastic, tested, and subsequently cleaned. The results were used to estimate both the bond strength and the adhesion energy (practical work of adhesion). Bond strength was computed as the ratio of the peak load divided by the cross-sectional area of the butt joint. Adhesion energy was computed as the area under the force–displacement curve divided by the cross-sectional area of the butt-joint specimen (Griffith, 1920). Comparisons were made between the moisture uptake and the adhesive strength as well as

Figure 2. Adhesion strength test set-up.

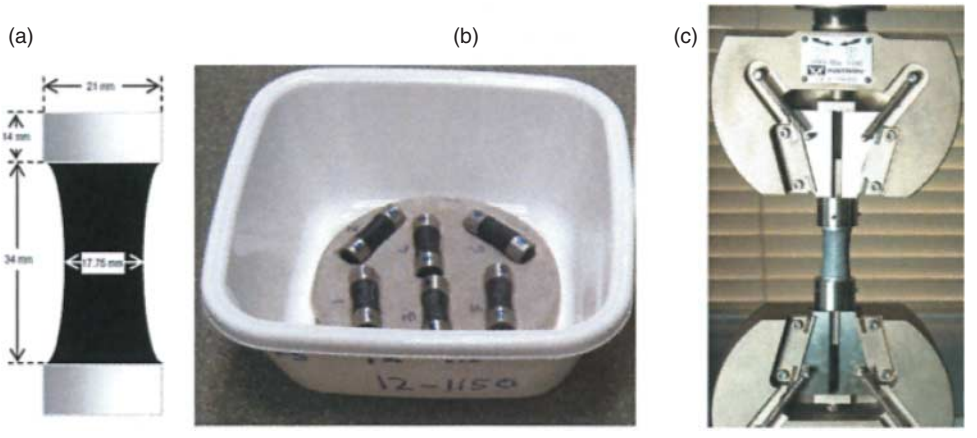


Figure 3. Asphalt mastic cohesive strength test. (a) Specimen dimensions, (b) samples in water bath, and (c) tensile strength test set.

the practical work of adhesion. The results also enabled a comparison between the thermodynamic work of adhesion and debonding, and the practical work of adhesion.

### 3.4. *Mastic cohesion tests*

#### 3.4.1. *Cohesion tests – specimen fabrication, conditioning, and testing*

Figure 3 shows details of the dog bone-shaped tensile specimens used to determine the cohesion (tensile strength) of the mastics. Also shown are the photograph of sample water baths used to moisture condition the mastics. Similar specimen configurations have been used by Kringos, Khedoe, Scarpas, and de Bondt (2011) to measure tensile strength of mastic. Samples were conditioned in water at 20°C for 112 days. Moisture uptake was computed using Equation (4). The results were used to estimate apparent diffusion coefficient. The moisture uptake results were also used to estimate the glass transition temperature using models proposed by Fox (1956). The latter calculations enabled a determination to be made about the level of plasticisation, if any, that occur during the 112 days of conditioning the mastics in water.

The samples were mechanically tested after five different moisture conditioning regimes: (1) completely dried samples about 2 weeks old, (2) after 112 days of soaking, (3) 112 days of storage in dry condition, (4) 112 days of soaking followed by 33 days of partial drying, and (5) 112 days

of soaking followed by 112 days of partial drying. To obtain the partially dried samples, samples of the 112 moisture-conditioned specimens were covered with plastic on all sides except the two ends so that water can evaporate from the ends only (Kringos et al. 2008). All the tensile tests were conducted at 20°C using a loading rate of 20 mm/min cross-head speed on an Instron machine (Figure 3(c)).

## 4. Results and discussion

### 4.1. *Aggregates – mineralogical composition*

Table 1 lists the mineralogical composition of the aggregates obtained from the Mineral Liberation Analyzer. The data shown are for the two aggregates used for manufacturing the mastics (Granite A and Limestone A) and also for the single aggregate type used as substrates during the adhesion testing (Granite B). The results show that the mineral compositions of the granite and limestone aggregates are significantly different in terms of the number and amount of mineral phases present. While the granites were made up of a large number of different dominant mineral phases (quartz, albite, potassium-dominant feldspar, and chlorite), the limestone consisted of predominantly (about 97%) calcite.

### 4.2. *Aggregates – physico-chemical properties*

Surface characteristics such as porosity, specific surface area, and SFE are key physico-chemical properties of aggregates that influence their adhesion to other materials. These properties could be obtained from gas sorption isotherms. The physico-chemical properties of samples of the aggregates were characterised using a dynamic sorption device (DVS Advantage), with octane as a probe to generate a series of sorption isotherms (Figure 4). The isotherms were obtained by measuring the amount of octane gas adsorbed across at relative pressures ranging from 5% to

Table 1. Mineral composition of aggregates.

| | Composition (%) | | |
|---|---|---|---|
| Mineral name | Granite A | Granite B | Limestone A |
| Quartz | 33.17 | 15.86 | – |
| Albite | 28.30 | 32.73 | – |
| *K*-feldspar | 16.93 | 9.64 | – |
| Chlorite | 11.90 | 13.52 | – |
| Muscovite | 4.58 | 3.43 | – |
| Other | 1.19 | 1.91 | |
| Epidote | 1.06 | 1.37 | – |
| Biotite | 1.00 | 0.34 | – |
| Anorthite | 0.82 | 18.54 | – |
| Calcite | 0.78 | 0.08 | – |
| Hornblende | 0.27 | 2.57 | – |
| Calcite | – | – | 96.98 |
| Dolomite | – | – | 1.30 |
| Clay | – | – | 0.93 |
| Quartz | – | – | 0.49 |
| Other | – | – | 0.30 |

Notes: K-feldspar, potassium-dominant feldspar; –, not applicable. Note that Granite B was used as the substrate during the adhesion testing.

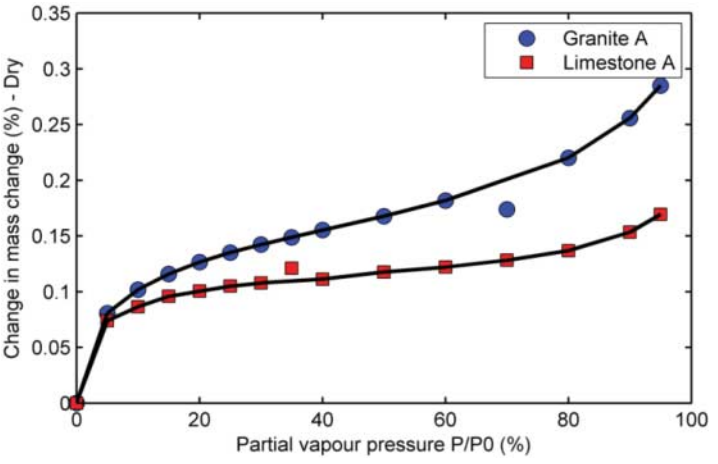


Figure 4. Octane sorption isotherms for aggregates (1.18 mm size fraction) used for fabricating mastics. Higher absorption for granite suggests that the aggregate is more porous than limestone.

95% at a constant temperature of 25°C. The absorption of octane was higher in the granite than in the limestone suggesting that the former is more porous (higher internal pores) than the latter. Also, as can be seen from Figure 4, the isotherms are similar to Type II isotherms. Therefore, the BET-specific surface area model is applicable. Additional detailed characterisation of the physico-chemical properties of the aggregates using sorption isotherms is provided elsewhere (Grenfell et al., 2013, 2014). From the latter study, the total SFE of the granite and limestone was reported as 353 and 223 $mJ/m^2$, respectively.

### 4.3. *Aggregate substrate moisture absorption*

Water uptake data were obtained for seven granite aggregate substrate specimens measuring 23-mm diameter by about 15 mm thick. Testing was limited to the granite because only this aggregate was used as the substrate for the adhesive strength tests. The average initial (dry) mass of the aggregate substrates was 15.61 g. The average 'equilibrium' moisture uptake at the end of tests was 0.491%. Figure 5 shows a sample moisture uptake versus the time plot for the aggregates. It can be seen from Figure 5 that for the aggregate considered, more than 90% of the equilibrium moisture uptake occurred during the first 24 h of water conditioning. This was typical for all the replicate samples tested.

Also shown in Figure 5 is the predicted moisture uptake obtained by using the Peleg model. As can be seen from Figure 5, there was an excellent agreement between the model predictions and the measured data. The model was employed to enable a direct comparison between moisture uptake and strength degradation in order to better quantify the effect of moisture. The corresponding Peleg model parameters (averaged) were 0.4720 and 2.0273 for $C_1$ and $C_2$, respectively. It is interesting to note the close agreement between the model-predicted equilibrium uptake of 0.493% (equal to reciprocal of $C_2$) and the experimentally determined equilibrium uptake of 0.491%.

The moisture uptake versus time data as well as the specimen dimensions were also used to determine apparent moisture diffusion coefficient (Equation (3) of the aggregate as 7350 $e^{-12}$ $m^2/s$.

### 4.4. *Mastic moisture absorption*

Moisture absorption was obtained for each of the four mastic types (LA + LF, LA + GF, GA + LF, and GA + GF). For each mastic type, at least six replicate specimens were tested. The average

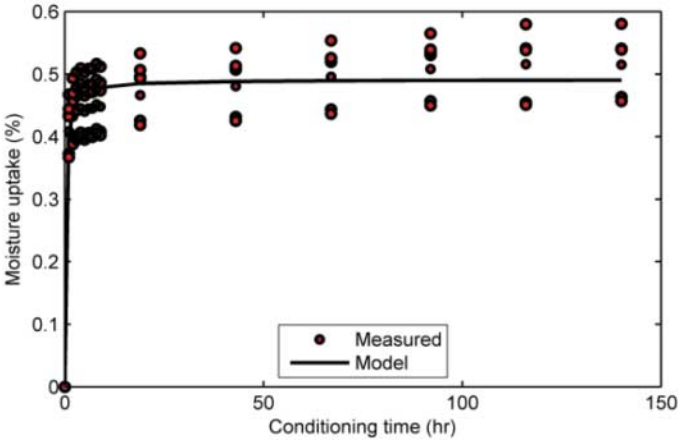


Figure 5. Water absorption in granite aggregate at 20°C. Excellent agreement between the Peleg model predictions and the measured data.

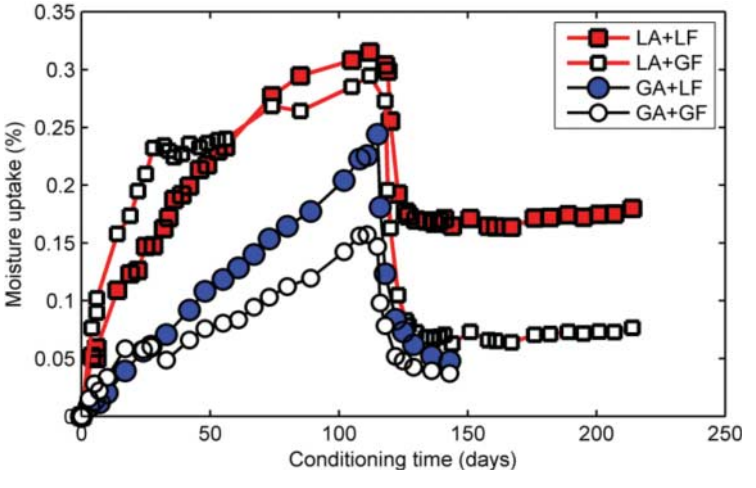


Figure 6. Moisture uptake of asphalt mastic containing different mineral aggregates and fillers. The sudden drop in moisture indicates the start of the drying phase after about 112 days of moisture conditioning. LA, limestone aggregate; LF, limestone filler; GA, granite aggregate; GF, granite filler.

dry weight of the mastic specimens at the beginning of testing was about 30 g. Figure 6 depicts the kinetics of the average water absorption for the four mastics. Compared with the aggregate substrates previously discussed, the rate of moisture uptake was slower with the time to reach equilibrium being significantly higher. In fact for most of the mastics, it appears that equilibrium could not be completely reached after 112 days of soaking in 20°C water. This compares with about a day for the aggregate substrates as previously discussed.

Differences in the rate and amount of water uptake could be seen based on fine aggregate and mineral filler type. For mastics containing the same aggregate type, absorption was higher in those with the granite filler. The lower moisture absorption in the mastic containing granite (aggregate and filler) could be due to the effect of material loss. It was noticed during the testing that the water containing granite mastics became much cloudier (a sign of material loss) than the limestone aggregate so the actual moisture uptake by the granite mastic could be underestimated.

Table 2. Moisture diffusion properties of mastics.

| Mix ID | $C_1$ | $C_2$ | $M_{eq}$(%)[a] | $D_{diff} \times 10^{-12}$ m$^2$/s | $m_{int}$ |
|---|---|---|---|---|---|
| LA + LF | 119.22 | 2.1 | 0.4768 | 3.1999 | 0.4801 |
| LA + GF | 42.91 | 3.19 | 0.1334 | 12.7629 | 0.4706 |
| GA + LF | 434.86 | 0.59 | 1.7065 | 0.2408 | 0.4872 |
| GA + GF | 256.56 | 4.41 | 0.2269 | 2.5526 | 0.4812 |

Notes: $M_{eq}$ may not be true equilibrium values as plot in Figure 6 shows that even after 112 days, the mastics were still absorbing substantial amounts of moisture. Also $M_{eq}$ may have been affected by weight loss, especially in the mastics containing granite.
[a]Values of $M_{eq}$ were determined based on the Peleg model.

In all cases, however, the lack of a plateau in the moisture uptake profiles suggests that none of the mastics achieved true equilibrium moisture after 112 days of moisture conditioning at 20°C.

Using the moisture uptake versus time data as well as the specimen dimensions as inputs to Equation (3), the apparent moisture diffusion coefficient was estimated. It must be noted that because of the specimen geometry, the application of Equation (3) to find moisture diffusion coefficient of the mastics is a gross simplification. Therefore, the computed diffusion coefficient should be considered tenuous and should only be used under conditions similar to those employed in this study. The Peleg model was used to fit the experimental data. The model parameters $C_1$ and $C_2$, equilibrium moisture uptake, as well as the computed diffusion coefficient of the bulk mastics are summarised in Table 2. Also shown in Table 2 is the interfacial moisture content computed using Equations (8)–(10). Because of the large disparity in moisture diffusion coefficient between the aggregate substrate (7350 e$^{-12}$ m$^2$/s) and the mastics (0.2408–12.76 e$^{-12}$ m$^2$/s), it appears that the amount of water at the interface of the aggregate–mastic bond was mainly influenced by the aggregate substrates' moisture content (Table 2). Future studies should consider simulation of interfacial moisture transport via the mastic as a way to better understand the effect of mastic film thickness on moisture sensitivity.

### 4.5. *Thermodynamic work of adhesion and debonding*

Table 3 lists the results of SFE components of the aggregate and bitumen. Also shown in Table 3 are thermodynamic work of adhesion ($TWA_{AB}$) and debonding in the presence of water ($TWD_{ABW}$) as well as the ratio between the two parameters, $ER_1$ proposed by Bhasin et al. (2006). Data from previous studies (Bhasin et al., 2006; Grenfell et al., 2013, 2014) suggest the durability and resistance to moisture damage of asphalt mixtures can be related to the magnitude of the $TWA_{AB}$ and $TWD_{ABW}$ as determined by $ER_1$. Aggregate–bitumen combinations with higher magnitudes of thermodynamic work of adhesion and lower work of debonding (i.e. higher $ER_1$ ratios) tend

Table 3. SFE and thermodynamic work of adhesion and debonding of aggregate–bitumen.

| | SFE components (mJ/m$^2$) | | | | | |
|---|---|---|---|---|---|---|
| Material | $\gamma^{LW}$ | $\gamma^{AB}$ | $\gamma^{T}$ | $TWA_{AB}$ (mJ/m$^2$) | $TWD_{AWB}$ (mJ/m$^2$) | $ER_1$ |
| Bitumen | 30.6 | 0.0 | 30.6 | N/A | N/A | N/A |
| Granite A | 67.8 | 284.0 | 352.5 | 131 | −109 | 1.20 |
| Limestone A | 75.2 | 147.0 | 222.7 | 128 | −51 | 2.51 |

Note: $TWA_{AB}$, thermodynamic work of adhesion between aggregate and bitumen; $TWD_{AWB}$, thermodynamic work of debonding aggregate-bitumen bond in the presence of water; N/A, not applicable.

to be more resistant to moisture-induced damage. The results show that for the aggregates and bitumen considered, the thermodynamic work of adhesion between bitumen and the two aggregates (granite and limestone) is comparable (131 and 128 $mJ/m^2$). However, the magnitude of the thermodynamic work of debonding (the reduction in free energy during debonding) for the two aggregates is significantly different resulting in lower $ER_1$ (worse moisture resistance) values for the granite–bitumen system compared with the limestone–bitumen combinations. It is important to note the significant difference between the bitumen intrinsic cohesive strength ($\gamma^T = 30.6\,mJ/m^2$) and the work of adhesion between aggregate and bitumen in the dry state (131 and 128 $mJ/m^2$ for granite and limestone, respectively). This is typical of the bond between a high surface energy material (in this case aggregate) and a low surface energy material (bitumen). Therefore, in the absence of moisture, the dominant failure mode in asphalt mixtures should be cohesive which is in accordance with common experience.

### 4.6. *Strength of aggregate butt joints – locus of failure*

The aggregate–mastic butt joint and moisture conditioning techniques adopted for this study were designed to ensure that failure occurred at the aggregate–mastic interface if indeed the interface has been degraded by the presence of water. This was accomplished by placing aggregate–mastic specimens with the bottom substrate partially submerged to ensure water enters aggregate–mastic interface before entering bulk mastic material as shown in Figure 1. The approach involved moisture conditioning of the butt-jointed specimens and tensile testing using a loading rate of 20 mm/min (Figures 1 and 2).

Figure 7 shows sample photographs of the fracture surface, taken immediately following a strength test, which could be used to characterise the locus of the fracture (i.e. the location of failure). Failure in the unconditioned specimens was mixed as both adhesive and cohesive failures were observed (Figure 7(a)). Clear adhesive failure with mastic completely debonded from the wet aggregate substrate was observed in all the mastic samples containing granite filler compared with no debonding in the limestone filler mastic. The results demonstrate that the loci of failure in the moisture-conditioned specimens were predominantly adhesive.

### 4.7. *Aggregate butt joints – moisture effects on mechanical properties*

Moisture conditioning at 20°C had a measurable effect on several mechanical properties of the aggregate–mastic butt joints, including the stress–strain behaviour, adhesive strength, and fracture energy.

Figure 8 shows the effect of increasing conditioning time on stress–strain behaviour of typical aggregate–mastic butt joints. Aggregate joints containing limestone (fine aggregate and mineral filler, LA + LF) performed best as moisture appears to have a negligible effect on the shape of the stress–strain curve. With the exception of limestone mastics, LA + LF, significant changes in the shape of the stress–strain curve were observed after 7 days of conditioning for all the aggregate–mastic joints. Thus, for the majority of the mastics that were tested, the effects of moisture conditioning were strength reductions (lower peak stress) and higher brittleness (lower strain at failure).

Figure 9 shows the effect of conditioning time on strength of the aggregate–mastic bond. The effect of moisture was negligible to slightly positive (i.e. slight increase in strength with time) in the case of mastics containing limestone fine aggregates irrespective of the filler type (Figure 9(a)). On the contrary, moisture effect was more pronounced in the mastics containing granite fine aggregates where strength decreased from about 4 MPa to about 1 MPa in seven days (Figure 9(b)). In this case, mastics containing granite aggregates lost about 20% and 80% of

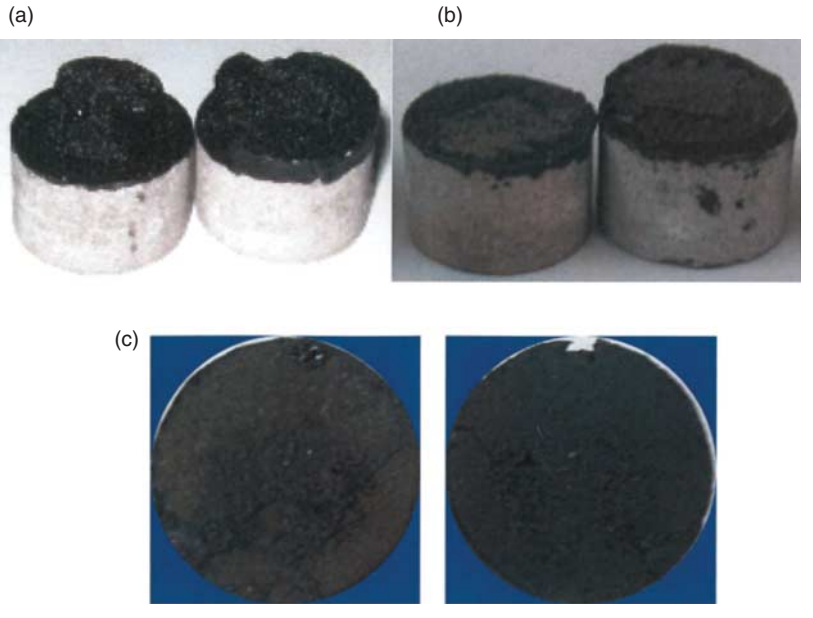


Figure 7. Loci of failure for moisture-induced damage in aggregate–asphalt mastic systems showing effect of conditioning time and aggregate type. (a) Mastic containing limestone aggregate and limestone filler (LA + LF) after 20 hours of moisture conditioning, (b) mastic containing granite aggregate and limestone filler (GA + LF) after 20 hours of moisture conditioning and (c) mastic GA + LF after three 168 hours of moisture conditioning. Stripping of mastic containing granite aggregates was more severe than limestone aggregate mastics.

their adhesion strength within the first 20 and 168 h, respectively (Figure 9(c)). The rapid loss of adhesive strength for short conditioning times observed in the granite mastics suggests poor water resistance and demonstrates the sensitivity of the various components of asphalt mixture to the presence of water. The results showing better resistance to moisture-induced damage for aggregate bonds containing limestone mastic than granite mastics is in agreement with previous studies (Airey & Choi, 2002; Airey et al., 2007) on more involved asphalt mixture testing. On this basis, it is reasonable to state that the butt-joint test set-up presented in this study offers a promising approach to evaluate moisture sensitivity of asphalt mixtures.

Results shown in Figures 7–9 demonstrate clearly the effect of conditioning time on aggregate–mastic bond strength. The results suggest a correlation between conditioning time and bond strength degradation may exist. A linear negative relationship was found between bond strength and square root of conditioning time (Figure 10) for the granite mastics. It should be noted that for the moisture conditioning test set-up used (Figure 1), the longer the conditioning time, the greater the amount of water that can diffuse through the aggregate substrate into the aggregate–mastic interface. This suggests that degradation of the aggregate–mastic bond strength is controlled in part by moisture diffusion.

### 4.8. *Aggregate butt joints – fracture energy*

The effect of moisture on the stress–strain curve as well as on bond strength could be captured using a single fracture energy parameter as a more elegant and unified way of characterising aggregate–mastic bond strength. In general, the larger the magnitude of fracture energy of a joint, the greater the resistance to failure from applied loading. As shown in Figure 11, one effect of moisture on

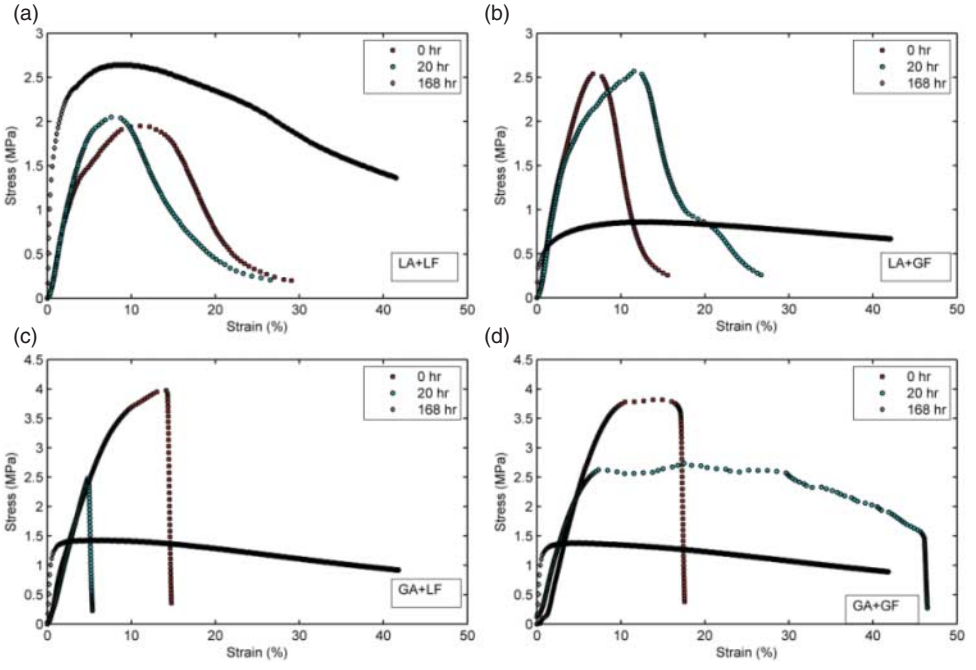


Figure 8. Effect of moisture conditioning time on stress–strain behaviour of aggregate–mastic butt joint. For majority of the mixtures, moisture conditioning resulted in strength reduction and increased brittleness. LA, limestone aggregate; LF, limestone filler; GA, granite aggregate; GF, granite filler.

aggregate–mastic bond strength is a reduction in fracture energy with conditioning time. The effect was more pronounced in mastics containing granite aggregates than those containing limestone aggregates. As shown in Figure 11(b), mastics containing granite aggregates retained only less than 10% of their original fracture energy after 168 h of moisture conditioning compared with about 80–100% in the case of limestone aggregate mastics.

The rapid loss of bond strength for short moisture conditioning times shown in Figure 11 is typical for adhesive joints with poor interfacial bond. The results show that the interfacial bond between aggregate–asphalt mastic weakens on exposure to moisture which is in accordance with the intrinsic bond strength calculated based on SFE measurements (Table 3). Thus, the ranking of moisture resistance of the mixtures based on the thermodynamic work of adhesion is comparable to the measured work of adhesion.

The significant loss in adhesive strength seen in Figure 11 after seven days of conditioning for the granite mastics could be explained using the physical adsorption theory and the nature of the mineral phases in the aggregates. In the case of physical adsorption, water attacks the adhesive–substrate interface by weakening the van der Waals interactions resulting in a reduction in the thermodynamic work of adhesion. For the aggregates considered, the dominant mineral phases of the granite (quartz, albite, etc.) could be used to explain the sensitivity of the granite mastic to water. Table 3 lists the thermodynamic work of adhesion and debonding. Based on the physical adsorption theory, if the thermodynamic work of adhesion is positive, then the bond is stable; a negative value suggests bond instability. It can be seen from Table 3 that in the dry condition, all aggregate–bitumen bonds exhibit positive work of adhesion (stable bonds) and negative values (unstable bonds) in the presence of moisture. The higher magnitude of the granite mixtures work of debonding compared with limestone suggest that the former is more sensitive to moisture

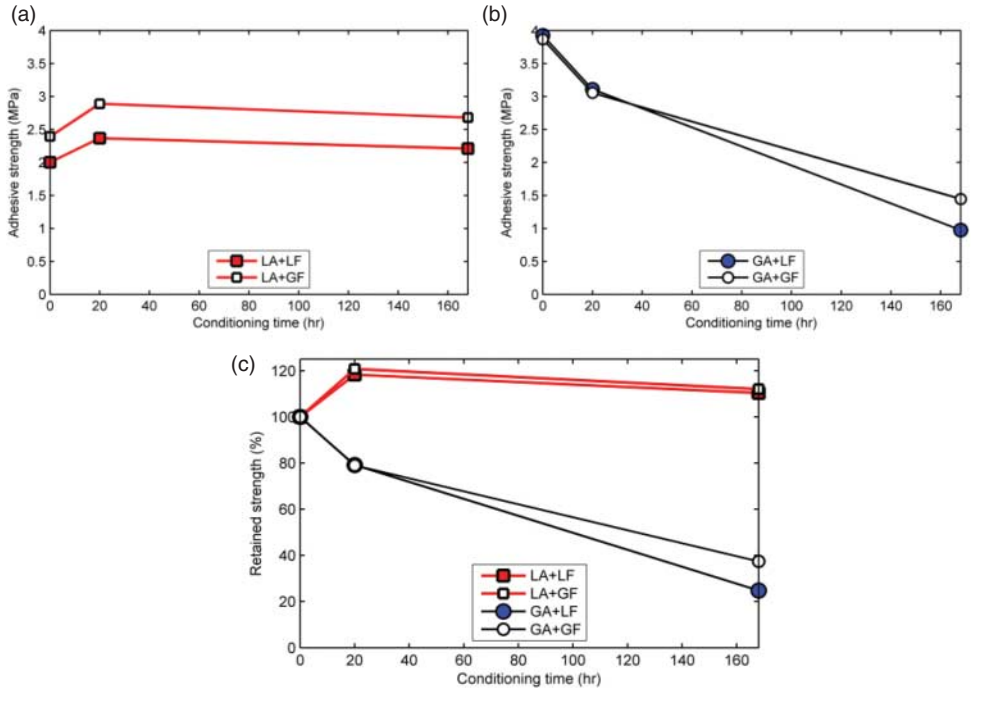


Figure 9. Effect of moisture conditioning time on bond strength of aggregate–mastic butt joints. Moisture caused negligible strength degradation in limestone aggregate mastics (a) compared to granite aggregate mastics (b). Mastics containing granite aggregates lost about 20% and 80% of their adhesion strength within the first 20 and 168 hours, respectively (c). LA, limestone aggregate; LF, limestone filler; GA, granite aggregate; GF, granite filler.

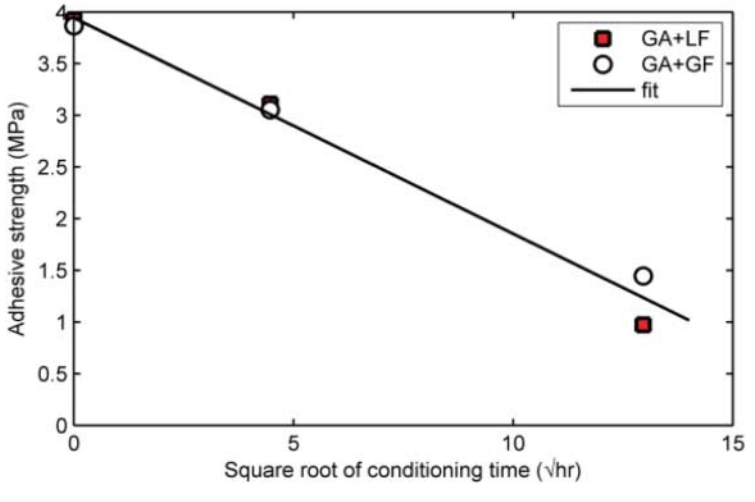


Figure 10. Relationship between aggregate-mastic bond strength and square root of conditioning time for mastic containing granite mastics. The excellent ($R^2 = 0.98$) linear fit between adhesive strength and square root of moisture conditioning time suggests a diffusion process controls mastic bond strength degradation. GA, granite aggregate; GF, granite filler; LF, limestone filler.

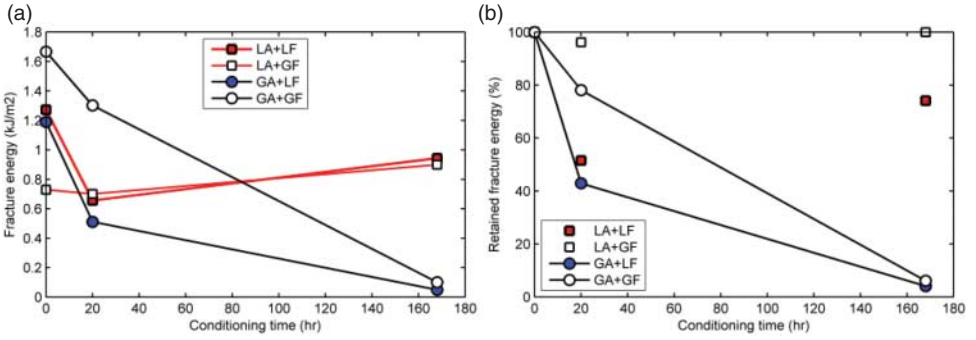


Figure 11. Effects of moisture conditioning on fracture energy of aggregate–asphalt mastic bond. Mastics containing granite aggregates retained only less than 10% of their original fracture energy after 168 hours of moisture conditioning compared to about 80–100% in the case of limestone aggregate mastics.

damage than the later which is in agreement with the practical work of adhesion obtained in this study. However, the negative sign in front of the work of debonding in the presence of water suggests all the aggregate–bitumen bonds, for the materials considered in this study, are unstable in the presence of water. The value of the $ER_1$ parameter (2.51) for limestone mastics bonds was higher than the $ER_1$ (1.20) for granite mastics, which is in agreement with mechanical test results.

### 4.9. *Effect of moisture uptake amount on bond strength*

As previously noted, the substrates used were fabricated from a single source/type of aggregate with unique mineralogical (Table 1) and physico-chemical properties (Figure 5 and Table 3). For instance, the aggregate demonstrated high moisture diffusivity ($7355 \times 10^{-12}$ m$^2$/s) and equilibrium water uptake (0.491%) at 20°C. The analyses using Equations (6)–(10) showed that the amount of moisture reaching the aggregate–mastic interface is mainly controlled by the diffusivity of the aggregate substrate. It is conceivable that different aggregate types will exhibit different moisture diffusion characteristics and, therefore, different moisture sensitivity. Under the same condition, a porous aggregate would absorb more moisture than a less porous aggregate over the same conditioning time. Therefore, moisture conditioning time alone may not completely describe the damage mechanism in aggregate–mastic joints. In this case, moisture concentration/uptake has been suggested as a more realistic parameter for characterising the effect of moisture on bond strength degradation. For this reason, finite element simulation can be used (Kringos et al., 2008, 2011) as a tool to determine moisture uptake at the aggregate–mastic interface in asphalt mixtures. For the purpose of the current paper, the Peleg model (Equation (6) together with Equation (10)) was used to estimate the variation of water uptake at the aggregate–mastic interface with time. This enabled a direct comparison between bond strength and moisture content (Figure 12) for the granite mastics that suffered significant strength degradation as a function of conditioning time. The correlation between moisture content and bond strength was found to be excellent as seen in Figure 13 where a plot of strength loss versus moisture content of the aggregate–mastic joint is depicted. Plots, such as Figure 13, might be useful in predicting critical moisture content for allowable levels of moisture damage in asphalt mixtures.

### 4.10. *Effect of re-using aggregate substrates on moisture absorption and bond strength*

At the beginning of this study, it was assumed that after a bond strength test, the aggregate substrates (original) could be cleaned with acetone and deionised water, dried and reused again

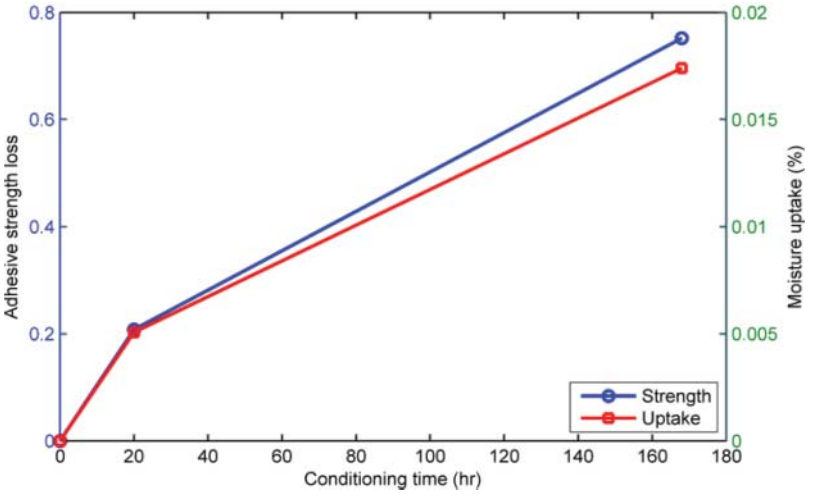


Figure 12. Aggregate–mastic adhesion strength loss versus moisture uptake and conditioning time for granite mastic GA + LF. Similar results were obtained for mastic GA + GF.

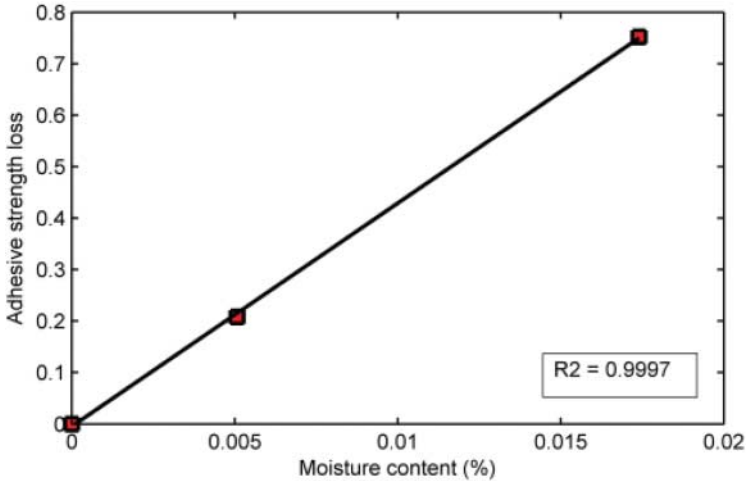


Figure 13. Correlation of moisture content of mastic with strength showing excellent correlation for GA + LF. Similar results were obtained for GA + GF.

(recycled). For this evaluation, two sets of aggregate substrates were considered. The first set comprises the 'original' or virgin substrates, while the second set comprises the acetone-cleaned 'recycled' aggregate substrates. As shown in Figure 14, moisture uptake profiles for the original and the recycled substrates are significantly different in terms of rate of moisture uptake as well as the magnitude of equilibrium moisture uptake. For instance, the original aggregates absorbed more than 90% of the final moisture uptake within the first 20 h compared with more than 46 h for the recycled substrates. The effects of the different moisture absorption are illustrated in Table 4 which shows that the adhesive strength for the original aggregate substrate is significantly lower than that of the recycled substrate after seven days of conditioning when they are compared. The use of a low SFE material like acetone (SFE $= 25\,\mathrm{mJ/m^2}$) to clean high SFE materials like aggregates could result in changes in the surface chemistry of the aggregates which combined

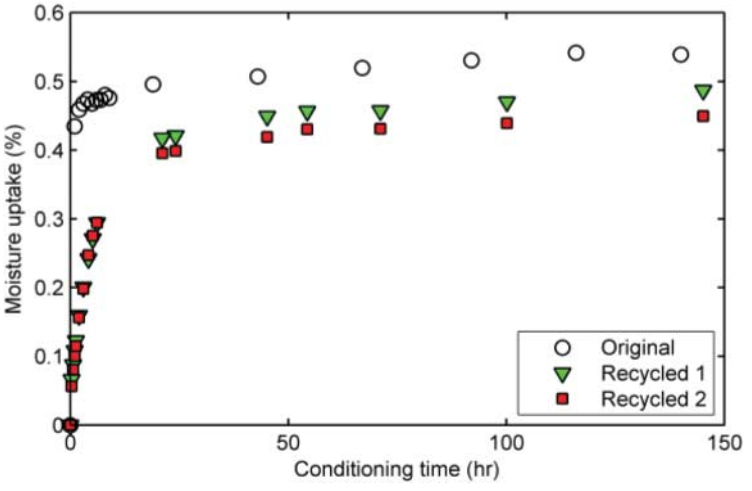


Figure 14. Effect of reusing aggregate substrates on moisture absorption.

Table 4. Effect of reusing aggregates substrates on mastic adhesive bond strength

| Mix ID | Substrate | Moisture uptake (%) | 7-day bond strength (MPa) |
|---|---|---|---|
| GA + LF | Original | 0.5592 | 0.9732 |
| | Recycled | 0.4691 | 3.7684 |
| GA + GF | Original | 0.5592 | 1.4460 |
| | Recycled | 0.4691 | 3.3265 |

Note: Lower moisture uptake by recycled substrate resulted in higher bond strength.

with the lower moisture absorption rate may have contributed to the unexpectedly high adhesion strength reported in Table 4. These results are limited but suggest that care may need to be taken during adhesion testing of moisture-conditioned samples if aggregates are to be cleaned and reused. Suggestions may include properly documenting the changes in the physico-chemical and moisture uptake characteristics of the aggregates that are reused or completely avoiding the use reuse of aggregates for adhesion testing altogether until a better understanding of the phenomenon is known.

### 4.11. *Mastic cohesive tensile strength – effect of conditioning time*

Figure 15 compares the cohesive strength of limestone (aggregate and mineral filler) mastics obtained from the dog bone-shaped tensile specimens that had been subjected to various moisture conditioning regimes ranging from soaking for up to 112 days followed by drying for the same length of time. Other conditioning regimes included storing the specimens at room temperature for 14 and 112 days. The 14-day storage simulated the freshly prepared specimens without any conditioning, while the storage at room temperature for 112 days provided baseline comparison for specimens that were submerged under water for 112 days. Three important effects of conditioning on mastic cohesive strength can be seen. First, long-term isothermal storage in air of asphalt mastic at room temperature (20°C and 50% RH) for 112 days did not result in significant changes in average cohesive tensile strength of the mastics containing limestone aggregate and mineral filler but caused more than 50% increase in strength for mastic containing granite fillers. These

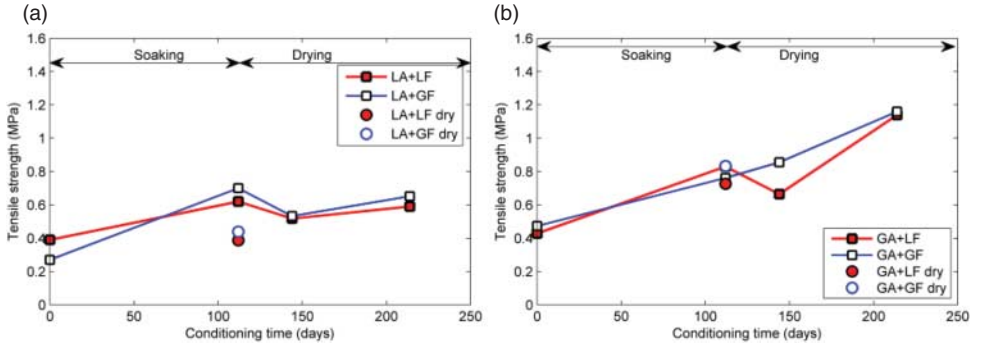


Figure 15. Effect of moisture conditioning at 20°C on cohesive strength of asphalt mastics. Tensile strength was obtained using a loading rate of 20 mm/min at a temperature of 20°C. (a) Limestone mastics and (b) granite mastics.

differences in strength changes could be attributed in part to isothermal ageing resulting from the stiffening effect of granite mineral fillers in the bitumen.

Second, the effect of long-term moisture conditioning (112 days at 20°C) on asphalt mastic is an increase in cohesive tensile strength. Mastics that had been conditioned in water for 112 days exhibited about 60% greater tensile strength than those stored dried. It is generally assumed that the effect of moisture on asphalt mixtures is a reduction in strength. Therefore, these results were not expected. One possible explanation is that amount of moisture absorbed by the mastic after 112 days was not enough to affect the cohesive strength of the mastic. This assertion is supported by data presented in Figure 6 where it can be seen that even after 112 days of soaking, none of the mastics studied showed any signs of reaching equilibrium moisture content. This increase in cohesive strength with moisture exposure has been reported in certain polymers where the phenomenon has been attributed to plasticisation.

Third, upon drying after 112 days of moisture conditioning, a slight decrease in tensile strength followed by some recovery of strength was observed. However, even after 112 days of drying, tensile strength of the 'partially' dried mastics was still lower than the 'fully wet' specimens. The initial drop in tensile strength just after removing the mastics from the water bath could be attributed to stress relaxation as the specimens were no longer submerged.

The lack of significant stiffness degradation observed in the mastics after 214 days of conditioning suggest, some other mechanism in addition to cohesive failure might be responsible for partially saturated asphalt mixtures. Also conditioning time alone might not be describing the effect of moisture on strength sufficiently well.

### 4.12. *Effect of moisture content on cohesive and adhesive strength*

The amount and the rate of moisture absorption were found to vary depending on mastic type. Therefore, the effect of conditioning time alone may not completely describe moisture sensitivity of the different mastics. In this case, the relationship between moisture content and strength may give a more useful description. Examples of two such plots are shown in Figures 16 and 17, for cohesive and adhesive strength, respectively.

From Figure 16, a positive correlation between moisture content and mastic cohesive strength is found. Since the mastics did not achieve equilibrium moisture (Figure 6), it is reasonable to expect that after a certain level of moisture uptake, the trend in the relationship between moisture will reverse. Such a behaviour has been reported for other materials (Bowditch, 1996) to describe cohesive failure and suggests plasticisation of a material by water and or internal stress

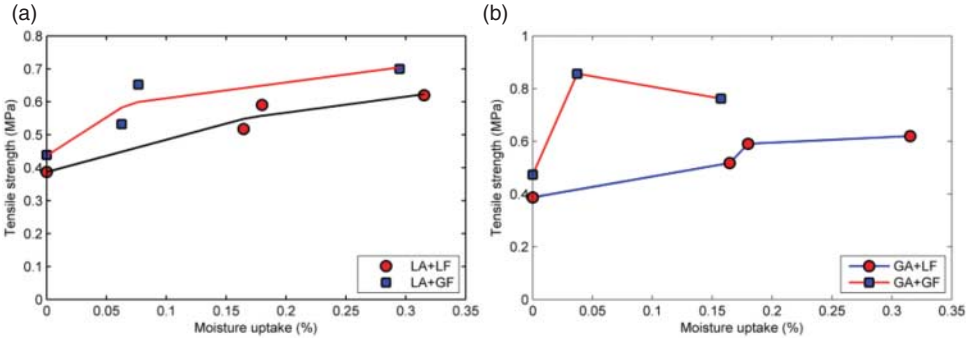


Figure 16. Effect of moisture uptake at 20°C on cohesive strength of asphalt mastics. (a) Data for asphalt mastics containing limestone aggregates and (b) data for asphalt mastics containing granite aggregates. Tensile strength was obtained using a loading rate of 20 mm/min at a temperature of 20°C.

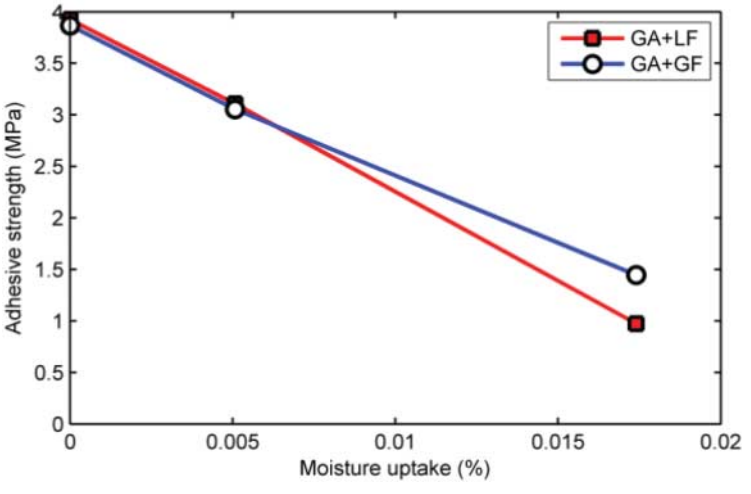


Figure 17. Effect of moisture uptake at 20°C on adhesive strength of asphalt mastics. Data for asphalt mastics containing granite aggregates. Tensile strength was obtained using a loading rate of 20 mm/min at a temperature of 20°C.

relaxation. It should be noted that even though plasticisation may lead to softening of an adhesive, in some cases at low moisture contents, moisture may actually lead to increased strength, which Figure 16(a) appears to show somewhat for the limestone mastics.

Considering the moisture uptake profiles for the four mastics considered in this study, the Fox equation (Equation (11) could be used to estimate changes in glass transition temperature of the mastics, where $T_g(m)$ and $T_g(w)$ are the glass transition temperatures of mastic and water and $p(m)$ and $p(w)$, the weight fractions of mastic and absorbed moisture after 112 days of soaking. Glass transition temperature for water was assumed to be −136°C, while that for the mastics was −20°C. Weight fraction of water in the mastic after 112 days of soaking was taken as $M_{eq}$ from Table 2. The results are presented in Table 5 where the biggest change in glass transition temperature was seen in the mastics containing granite aggregate and granite filler where there was a 3.6 degree drop in glass transition temperature. Drop in glass transition temperature is an indication of plasticisation. The results thus appear to show that some plasticisation can occur in the mastics as a result of moisture conditioning. Because of the empirical nature of Equation (11), additional

Table 5. Effect of moisture conditioning on estimated asphalt–mastic glass transition temperature.

| Mix ID | $M_{eq}$ (%) | $T_g$ (w) (°C) | $T_g$ (m) (°C) | $p(w)$ | $p(m)$ |
|---|---|---|---|---|---|
| LA + LF | 0.48 | −136 | −20 | 0.00477 | 0.99523 |
| LA + GF | 0.13 | −136 | −20 | 0.00133 | 0.99867 |
| GA + LF | 1.71 | −136 | −20 | 0.01710 | 0.98290 |
| GA + GF | 0.23 | −136 | −20 | 0.00227 | 0.99773 |

studies may be required. However, the trends in the computed glass transition temperature are in agreement with the data presented in Figure 16. As additional evidence for the occurrence of plasticisation, Equation (5) could be used assuming relative permittivity values of 4.3 and 7 for the dry unconditioned mastics and 7 for the moisture-conditioned ones. In this case, the predicted drop in strength of about 60% was obtained as a result of moisture conditioning

$$\frac{1}{T_g} = \frac{p(w)}{T_g(w)} + \frac{p(m)}{T_g(m)}. \tag{11}$$

In contrast to the effect of moisture on cohesive strength of mastics, a trend of decreasing adhesive tensile strength with moisture was found (Figure 17). A major difference between the failure mode in Figure 16 and that in Figure 17 is that the rate of strength degradation with moisture uptake is an order of magnitude higher for adhesive strength than for cohesive strength. The results appear to be in general agreement with previous studies that suggested that the amount of water molecules required for interfacial failure of aggregate–bitumen bonds is in the order of 35–45 nm thick (Nguyen et al., 1995). The results suggest that the effect of moisture on adhesive strength is more detrimental than the effect of moisture on cohesive strength. It is important to remember, however, that the nature of the experimental set-up for conditioning the adhesive butt joints (Figure 1) meant that moisture diffusion into the aggregate–mastic interface through the uncoated aggregate was faster than through the bulk mastic. Future study focused on simulating moisture diffusion to the aggregate–mastic interface via the bulk mastic may be warranted.

## 5. Conclusions

The objective of this paper was to investigate the effect of moisture on the strength of aggregate–mastic bonds using tensile butt joints and dog bone-shape tensile specimens fabricated from four different mastics and subjected to various moisture conditioning regimes. The following conclusions were reached based on the data presented in the paper:

From the analyses conducted in this study, the following are recommended:

- Moisture-induced degradation of the aggregate–mastic bond strength is influenced by aggregate type and conditioning time. Aggregate–mastic joints with the mastics containing granite aggregate lost 20% and 80% of their adhesion strength within the first 20 and 160 h, respectively. Mastics containing limestone aggregates, on the other hand, retained over 100% of their initial adhesive strength over the same period.
- Results of mineralogical analyses suggest that the worse moisture resistance of the granite mastics compared with the limestone mastic bonds could be explained, in part, by the dominant mineral phases in the granite. The three dominant minerals in granite, namely albite, feldspar, and quartz have been associated with poor adhesion and interfacial failure in bitumen–aggregate bonds in previous studies.

- There was excellent correlation between the interfacial moisture content and strength. Plots of strengths against the square root of conditioning time were linear suggesting a diffusion process controls the moisture-conditioned aggregate-mastic bond strength.
- A good correlation was found between the thermodynamic work of adhesion and debonding, and the practical work of adhesion of the aggregate–mastic bonds. This suggests that physical adsorption controls the moisture damage in aggregate–mastic bonds.
- The presence of moisture at the aggregate–mastic interface was associated with significant strength degradation and increased brittleness, which was mastic specific. Given that the same aggregate substrate was used, it can be concluded that moisture-induced strength degradation of the aggregate–mastic bond are influenced by both physico-chemical characteristics and mineralogical composition of the asphalt components.
- The interfacial bond between aggregate and asphalt mastic weakens on exposure to moisture which is in accordance with the intrinsic bond strength calculated based on SFE measurement. The effect of moisture on the aggregate–mastic interfacial bond appears to be more detrimental than the effect on the bulk mastic.
- The technique, based on tensile butt joints and simulated interfacial moisture conditioning, developed in this study appears to be promising for rapidly evaluating moisture sensitivity of asphalt mixtures in the laboratory.
- The current study simulated moisture transport to the aggregate–mastic interface via the aggregate substrate. Future studies focused on simulating moisture diffusion to the aggregate–mastic interface via the mastic layer are warranted.

## Funding

The funding for this project was provided in part by the UK Engineering and Physical Sciences Research Council (EPSRC).

## References

Airey, G. D., & Choi, Y. K. (2002). State of the art report on moisture sensitivity test methods for bituminous pavement materials. *Road Materials and Pavement Design, 3*(4), 355–372.

Airey, G., Masad, E., Bhasin, A., Caro, S., & Little, D. N. (2007, June). Asphalt mixture moisture damage assessment combined with surface energy characterization. In A. Loizos, T. Scarpas, and I. Al-Quadi (Eds.), *Advanced characterization of pavement and soil engineering materials* (pp. 739–748). London, England: Taylor & Frances Group.

Apeagyei, A. K., Grenfell, J. R. A., & Airey, G. D. (2013). Evaluation of moisture sorption and diffusion characteristics of asphalt mastics using manual and automated gravimetric sorption techniques. *Journal of Materials in Civil Engineering*. doi:10.1061/(ASCE)MT.1943-5533.0000929

Arambula, E., Caro, S., & Masad, E. (2010). Experimental measurement and numerical simulation of water vapor diffusion through asphalt pavement materials. *Journal of Materials in Civil Engineering, 22*(6), 588–598.

Bell, L. N., & Labuza, T. P. (2000). *Moisture sorption: Practical aspects of isotherm measurements and use*. St. Paul, MN: American Association of Cereal Chemists.

Bhasin, A., Masad, E., Little, D. N., & Lytton, R. L. (2006). Limits on adhesive bond energy for improved resistance of hot-mix asphalt to moisture damage. *Transportation Research Record* 1970, 3–13.

Bottcher, C. J. (1973). *Theory of electric polarization, Vol. 1: Dielectrics in static fields*. New York: Elsevier.

Bowditch, M. R. (1996). The durability of adhesive joints in the presence of water. *International Journal of Adhesion and Adhesives, 16*, 73–79.

Caro, S., Masad, E., Bhasin, A., & Little, D. (2008). Moisture susceptibility of asphalt mixtures, part 1: Mechanisms. *International Journal of Pavement Engineering, 9*(2), 81–98.

Chang, C., Chen, J., & Wu, T. (2011). Dielectric modeling of asphalt mixtures and relationship with density. *Journal of Transportation Engineering, ASCE, 137*(2), 104–111.

Comyn, J. (1983). *Durability of structural adhesives*. (A. J. Kinloch, Ed.), New York: Applied Science.

Comyn, J. (2005). Environmental (durability) effects. In R. D. Adams (Ed.), *Adhesive bonding: Science, technology and applications* (pp. 123–142). Boca Raton, FL: CRC Press.

Crank, J. (1975). *The mathematics of diffusion* (2nd ed., p. 414). New York: Oxford University Press.

Evans, R., Frost, M., Stonecliffe-Jones, M., & Dixon, N. (2007). Assessment of the in-situ dielectric constant of pavement materials. *Transportation Research Record*, 2037, 128–135.

Fox, T. G. (1956). Influence of diluents and of copolymer composition on the glass temperature of a polymer system. *Bulletin of the American Physical Society, 1*, 123–132.

Grenfell, J. R. A., Ahmad, N., Liu, Y., Apeagyei, A. K., Airey, G. D., & Large, D. (2014). Assessing asphalt mixture moisture susceptibility through intrinsic adhesion, bitumen stripping and mechanical damage. *Road Materials and Pavement Design, 15*(1), 131–152.

Grenfell, J. R. A., Ahmad, N., Liu, Y., Apeagyei, A. K., Airey, G. D., & Large, D. (2013). Application of surface free energy techniques to evaluate bitumen aggregate bonding strength and asphalt mixture moisture sensitivity. *ICE Construction.* doi:10.1680/coma.13.00003

Griffith, A. A. (1920). The phenomena of flow and rupture in solids. *Philosophical Transactions of the Royal Society of London, Series A, 221*, 163–198.

Kassem, E. A., Masad, E., Bulut, R., & Lytton, R. L. (2006). Measurements of moisture suction and diffusion coefficient in hot-mix asphalt and their relationships to moisture damage. *Transportation Research Record*, 1970, 45–54.

Kringos, N., Khedoe, R., Scarpas, A., & de Bondt, A. (2011). *A new asphalt concrete moisture susceptibility test methodology*. Washington, DC: Transportation Research Board Annual Meeting.

Kringos, N., Scarpas, A., & deBondt, A. (2008). Determination of moisture susceptibility of mastic-stone bond strength and comparison to thermodynamical properties. *Journal of the Association of asphalt Paving Technology*, 77, 435–478.

Nguyen, T., Byrd, E., Alsheh, D., & Bentz, D. (1995). *Relation between adhesion loss and water at the polymer/substrate interface*. Proceedings adhesion society meeting, Hilton Head Island, SC, USA.

Peleg, M. (1988). An empirical model for the description of moisture sorption curves. *Journal of Food Science, 53*(4), 1216–1219.

Saarenketo, T. *Measuring electromagnetic properties of asphalt for pavement quality control and defect mapping*. Retrieved July 24, 2013, from http://www.vegagerdin.is/nvf33.nsf/0/6423655ed26a5bd400256de90031ecaf/$FILE/Asphalt_electromagnetics_TimoS_030603.pdf

Sihvola, A. H. (1999). *Electromagnetic mixing formulas ansd applications*. London: Institution of Electrical Engineers.

Vasconcelos, K. L., Bhasin, A., Little, D. N., & Lytton, R. L. (2011). Experimental measurement of water diffusion through fine aggregate mixtures. *Journal of Materials in Civil Engineering, 23*(4), 445–452.

Vlachovicova, Z., Stastna, J., & Zanzotto, L. (2003). Shear viscosity and dielectric permittivity on asphalt modified by SBS. *Petroleum and Coal, 45*(3–4), 178–183.

Wake, W. C. (1978). Theories of adhesion and uses of adhesives: A review. *Polymer, 19*(3), 291–308.